ISSN 2472-1972

Portal Venous Metabolite Profiling After RYGB in Male Rats Highlights Changes in Gut-Liver Axis

Margaret A. Stefater[1], Julian A. Pacheco[2], Kevin Bullock[2], Kerry Pierce[2], Amy Deik[2], Enju Liu[3], Clary Clish[2], and Nicholas Stylopoulos[1,3]

[1]Division of Endocrinology, Department of Pediatrics, Boston Children's Hospital, Harvard Medical School, Boston, Massachusetts 02115; [2]Broad Institute of MIT and Harvard, Cambridge, Massachusetts 02142; and [3]Institutional Centers for Clinical and Translational Research, Boston Children's Hospital, Boston, Massachusetts 02115

ORCiD numbers: 0000-0003-4767-868X (M. A. Stefater).

After Roux-en-Y gastric bypass (RYGB) surgery, the intestine undergoes structural and metabolic reprogramming and appears to enhance use of energetic fuels including glucose and amino acids (AAs), changes that may be related to the surgery's remarkable metabolic effects. Consistently, RYGB alters serum levels of AAs and other metabolites, perhaps reflecting mechanisms for metabolic improvement. To home in on the intestinal contribution, we performed metabolomic profiling in portal venous (PV) blood from lean, Long Evans rats after RYGB vs sham surgery. We found that one-carbon metabolism (OCM), nitrogen metabolism, and arginine and proline metabolism were significantly enriched in PV blood. Nitrogen, OCM, and sphingolipid metabolism as well as ubiquinone biosynthesis were also overrepresented among metabolites uniquely affected in PV vs peripheral blood in RYGB-operated but not sham-operated animals. Peripheral blood demonstrated changes in AA metabolism, OCM, sphingolipid metabolism, and glycerophospholipid metabolism. Despite enrichment for many of the same pathways, the overall metabolite fingerprint of the 2 compartments did not correlate, highlighting a unique role for PV metabolomic profiling as a window into gut metabolism. AA metabolism and OCM were enriched in peripheral blood both from humans and lean rats after RYGB, demonstrating that these conserved pathways might represent mechanisms for clinical improvement elicited by the surgery in patients. Together, our data provide novel insight into RYGB's effects on the gut-liver axis and highlight a role for OCM as a key metabolic pathway affected by RYGB.

Key Words: Portal vein, metabolomics, Roux-en-Y gastric bypass (RYGB), bariatric surgery, diabetes, intestine

1. Introduction

One of the most remarkable features of Roux-en-Y gastric bypass surgery (RYGB) that makes it a superior therapy to other interventions is its ability to elicit clinically significant weight loss that is sustained over long periods of time [1, 2]. Additionally, 70% to more than 90% [3-5] of patients with type 2 diabetes (T2D) who undergo RYGB experience remission. Multiple hypotheses have been put forward regarding the mechanisms behind these beneficial effects

Abbreviations: AA, amino acids; DMG, dimethylglycine; FDR, false discovery rate; NAFLD, nonalcoholic fatty liver disease; OCM; one-carbon metabolism;OEA, oleoylethanolamide; PCA, principal components analysis; PV, portal vein; RYGB, Roux-en-Y gastric bypass; T2D, type 2 diabetes; VIP, variable importance in projection.

Received 27 November 2019
Accepted 21 January 2020
First Published Online 23 January 2020
Corrected and Typeset 20 February 2020

of the surgery, including a role for enteroendocrine signaling [6-8], alterations to the intestinal microbiome [9-11], and augmented intestinal energy use [12]. In particular, after RYGB, the intestine exhibits evidence of structural and metabolic reprogramming that appears to enhance use of energetic fuels including glucose and amino acids (AAs) [12, 13].

A substantial number of prior studies have demonstrated significant changes in peripheral blood levels of metabolites, including AAs [14-18], sphingolipids [15, 19], tricarboxylic acid (TCA) cycle intermediates [19], and fatty acids [15, 18, 19] in human patients and in rodents. As a direct conduit between the intestine's mesenteric drainage and the liver, the portal vein (PV) is the major source of hepatic venous blood supply. In addition to intestinal metabolic reprogramming, RYGB elicits dramatic alterations in hepatic gene expression that suggest a shift in metabolic substrate use in the liver [20-22]. We performed untargeted metabolite profiling in PV blood using a liquid chromatography mass spectrometry (LC/MS)-based approach, which can delineate thousands of metabolites simultaneously, to isolate the effects of RYGB on metabolites within the gut-liver axis. This was performed in lean, RYGB-operated rodents to identify metabolites altered as a result of the surgery itself, rather than to obesity treatment.

2. Materials and Methods

A. Animals

The animal experiments and animal care were performed in compliance with and were approved by the Boston Children's Hospital Institutional Animal Care and Use Committee. Male Long Evans rats were used for the studies. Animals were individually housed and were maintained on 12-hour light, 12-hour dark cycle (lights on at 7 AM) in facilities with an ambient temperature of 19°C to 22°C and 40% to 60% humidity.

B. Rodent Surgical and Postsurgical Procedures

Animals were fasted overnight before surgery. Seven RYGB and 5 sham operations were performed. During the surgical procedures, rats were maintained on inhalation anesthesia (isoflurane 1%-4%). Rats were fasted for the first 24 hours after the surgery. After evaluating the health and behavior of each animal, a liquid diet was reintroduced 48 to 72 hours following the operation. Beginning on postoperative day 7, the rats were switched to their preoperative diet. To achieve comparable body weight in RYGB- and sham-operated animals, and to mitigate the higher postoperative body weight gain classically observed in sham-operated rats, we restricted the food intake of sham-operated animals during the postoperative phase.

C. Roux-en-Y Gastric Bypass

The total length of the small intestine was measured, the ligament of Treitz was identified, and the jejunum was divided at the appropriate distance downstream of this ligament. An end-to-side jejuno-jejunostomy and a gastrojejunostomy were created with a 7-0 silk or Prolene (Ethicon, Inc.) running suture. A pouch was created by transecting the stomach. The gastric artery was preserved and only the small vascular branches were cauterized. The laparotomy was closed with a 5-0 polydioxanone (PDS) suture in 2 layers. After surgery, body weight was recorded at least twice weekly.

D. Sham Surgery

A laparotomy was performed, as in RYGB surgery. Then, a loop of jejunum was divided and subsequently repaired with suture. The skin was closed in 2 layers. The postoperative recovery and observation were performed exactly as described for RYGB animals.

E. Blood Collection

Following a 4-week postsurgical recovery period, animals were fasted overnight. Animals were euthanized with CO_2. Portal blood was collected via syringe using a 27-gauge needle. Peripheral blood was collected by aortic puncture.

F. Analysis

LC/MS-based analytical methods were used to measure the metabolome in serum from portal and peripheral blood, as described previously [23]. These methods included C8-positive (lipids and nonpolar metabolites lipids of known identity and thousands of unknown peaks), C18-negative (free fatty acids, eicosanoids, bile acids, and metabolites of intermediate polarity), hydrophilic interaction liquid chromatography (HILIC)-positive (AAs, AA metabolites, acylcarnitines, dipeptides, and other cationic polar metabolites), IC-negative (intermediates in the glycolytic pathway, TCA cycle, organic acids, and thousands of unknown peaks) and HILIC-negative (sugars, organic acids, purines, pyrimidines, and other anionic polar metabolites). Coefficient of variation for each assayed metabolite is included in supplemental data (available at doi.org/10.6084/m9.figshare.11223302 [24]). Internal standards used are listed as follows:

HILIC-negative: inosine-^{15}N4, thymine-d4, and glycocholate-d4 (Cambridge Isotope Laboratories)
C18-negative: 15R-15-methyl PGA2, 15S-15-methyl PGD2, 15S-15-methyl PGE1, 15S-15-methyl PGE2, 15R-15-methyl PGF2a
HILIC-positive: valine-d8, phenylalanine-d8 (Cambridge Isotope Laboratories)
C8-positive: C24:0 PC (1-dodecanoyl-2-tridecanoyl-sn-glycero-3-phosphocholine; Avanti Polar Lipids)

G. Human Data

We reanalyzed untargeted metabolomic data (available at doi.org/10.6084/m9.figshare.8053553.v1 [24]) generated by LC/MS from obese patients who had undergone RYGB more than 6 months before blood collection, vs obese control patients [24]. This was compared to metabolomic profiling from rodent peripheral blood. Human samples were reflective of the general bariatric surgery population and were mostly female; detailed demographics are available in the original publication.

H. Statistics

Basic statistical comparisons and pathway and enrichment analyses of the collected metabolomics datasets were performed with Metaboanalyst, which uses known HMDB-labeled metabolites. We used logarithmic transformation and autoscaling of the data (raw values were mean-centered and divided by the SD of each variable). *P* values were adjusted using the original method of Benjamini and Hochberg, and for t tests, *P* values of less than 0.05166144201 were defined as "discoveries" based on a false discovery rate (FDR) of less than .05. A table of raw and adjusted *P* values can be found in the data repository accompanying this paper (available at doi.org/10.6084/m9.figshare.11223302 [24]). Prism 7 (GraphPad) was used for graphs. SAS version 9.4 and SPSS version 24 were used for the principal component and the correlation and regression analyses.

3. Results

A. Rodent Peripheral Serum Metabolomic Profiles Reveal Weight-Independent Roux-en-Y Gastric Bypass–Affected Metabolites

To uncover metabolites affected in a weight-independent manner after RYGB, we performed metabolomic profiling in peripheral and portal blood from lean, RYGB-operated rats as compared

with sham-operated controls. Rats, which were lean before surgical intervention, neither gained nor lost significant weight across the course of the study (Fig. 1A), and by the end of the study there was no difference in body weight of sham-operated vs RYGB-operated animals (Fig. 1B).

A total of 405 metabolites were detected in peripheral blood. Of these, 76 metabolites were found to be significantly enriched or depleted in peripheral blood from RYGB- vs sham-operated animals. Among these weight-loss independent metabolites, the gluconeogenic AAs, alanine, glycine, phenylalanine, and tyrosine were increased after RYGB, whereas asparagine and serine were depleted relative to sham-operated animals (Fig. 2A). Serine is an important methyl donor for the production of methyl-tetrahydrofolate, and this process generates glycine. The methyl donor choline and its byproduct, dimethylglycine (DMG), were notably also among the most-enriched metabolites in peripheral blood after RYGB (Fig. 2B). Triacylglycerides (TAG) and diacylglycerols species were variably enriched or depleted in peripheral blood after RYGB, perhaps reflecting enhanced fat turnover after surgery that is weight independent (Fig. 2C).

Pathway analysis of differentially affected metabolites demonstrated significant enrichment of several processes including those relevant to nitrogen metabolism, one-carbon metabolism (OCM), oxidative phosphorylation (ubiquinone and other terpenoid-quinone biosynthesis), TCA cycle anapleurosis, and sphingolipid metabolism (Fig. 2D).

We performed principal components analysis (PCA; Fig. 2E) to reduce our data set into smaller metabolite lists descriptive of the whole dataset. Of 396 metabolites detected in all 12 animals, we identified 11 PCs describing the variance in our data (Fig. 2F), and using the 11-factor solution we compared scores for RYGB- vs sham-operated animals, finding a significant difference for PC1 (P = .008). Metabolites were assigned to a PC if loadings exceeded that for the other 11 PCs. PC1 was enriched for sphingolipid metabolism, glycerophospholipid metabolism, phenylalanine, tyrosine, and tryptophan biosynthesis, β-alanine metabolism, and glycine/serine/threonine metabolism (Fig. 2G). Partial least squares discriminant analysis (PLS-DA) was next used to identify those metabolites most highly contributing to the separation between RYGB and sham fingerprints in peripheral blood (Fig. 2H). This demonstrated 155 metabolites with variable importance in projection (VIP) scores greater than 1.0. The top 15 are shown in Fig. 2I; the methyl donor, choline, was among the top metabolites separating RYGB and sham fingerprints.

B. Portal Venous Blood Exhibits a Unique Metabolite Fingerprint Reflecting Intestinal Metabolic Reprogramming by Roux-en-Y Gastric Bypass

In PV blood, we detected 405 unique metabolites, of which 48 were significantly depleted or enriched in RYGB-operated animals as compared with sham-operated animals (Fig. 3A and

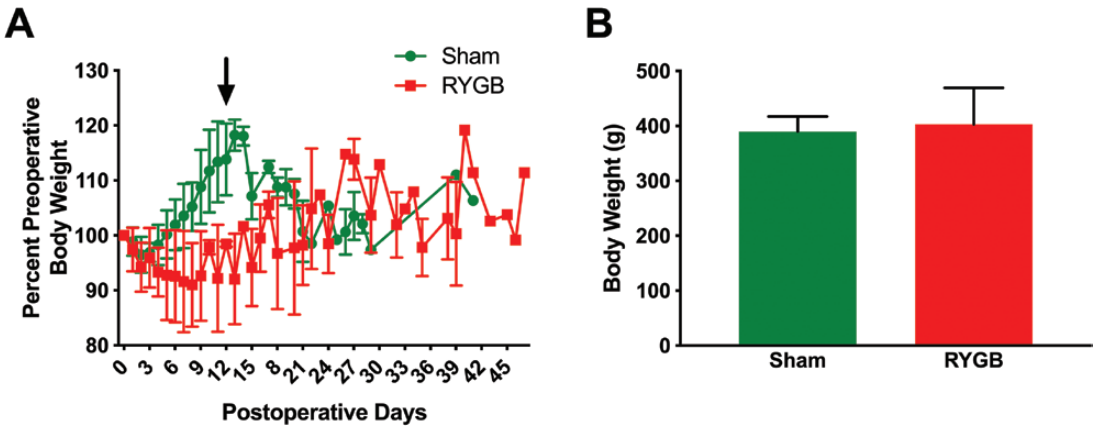

Figure 1. Body weight of Roux-en-Y gastric bypass (RYGB)- and sham-operated rats A, across time and B, at time of blood sampling. Arrow in A indicates when weight-matching paradigm began.

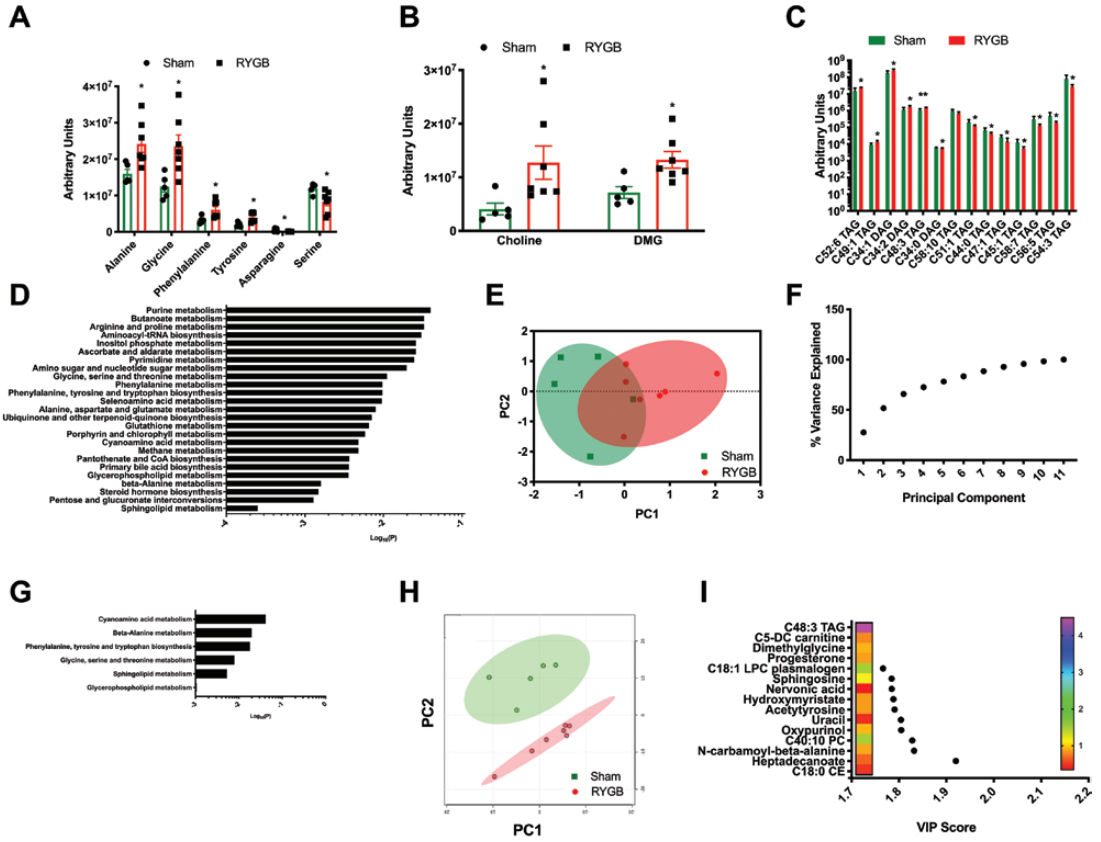

Figure 2. Peripheral blood metabolite profiling. A, Gluconeogenic amino acids, alanine, glycine, phenylalanine, and tyrosine were increased, whereas asparagine and serine were increased in peripheral blood after Roux-en-Y gastric bypass (RYGB) relative to lean controls. B, Choline and dimethylglycine (DMG) levels were increased by RYGB. C, Concentrations of triacylglycerides (TAGs) and diacylglycerols (DAGs) after RYGB. D, Pathways describing changes in the peripheral metabolome after RYGB. E, Principal components analysis (PCA) scores plot and F, scree plot representing peripheral blood samples from RYGB- and sham-operated animals. G, Significant pathways represented by PC1 metabolites in peripheral blood. H, Partial least squares discriminant analysis (PLS-DA) scores plot demonstrating separation of groups primarily along PC1. I, Top 15 metabolites identified by PLS-DA as key discriminating metabolites between the 2 experimental groups (ie, with highest variable importance in projection [VIP] scores). Heat map shows $\log_2$ fold-change in identified metabolites, and all were significant as defined by P less than .05.

3B). Weight-independent metabolites enriched after RYGB included the methyl donor betaine and its metabolite, DMG (Fig. 3C and 3D). The lipid messenger N-oleoylethanolamide (OEA) was depleted (Fig. 3E), as were several species of acylcarnitines (Fig. 3F), pointing to changes in intestinal lipid metabolism after RYGB. Nitrogen metabolism and OCM were identified among significantly enriched pathways (Fig. 3G).

After excluding metabolites not measurable in PV blood from all rats included in the study, we performed a PCA of 295 remaining metabolites. As was true in peripheral blood, there was considerable overlap in the fasting metabolomic profile of portal blood from RYGB- and sham-operated animals (Fig. 4A). However, heat maps for known (Fig. 3B) and unknown (Fig. 4F) metabolites demonstrate clearly that PV blood exhibits a distinct metabolomic phenotype. Of 11 PCs explaining 100% of the variance in the metabolite levels measured in portal blood (Fig. 4B), PC scores for PC2 were significantly lower in RYGB- than sham-operated animals (P = .02). PC2 associated most strongly with 48 metabolites and, based on these, 3 pathways were identified as significantly enriched, including glycine/serine/threonine metabolism (Fig. 4C). PLS-DA (Fig. 4D) identified 106 metabolites with

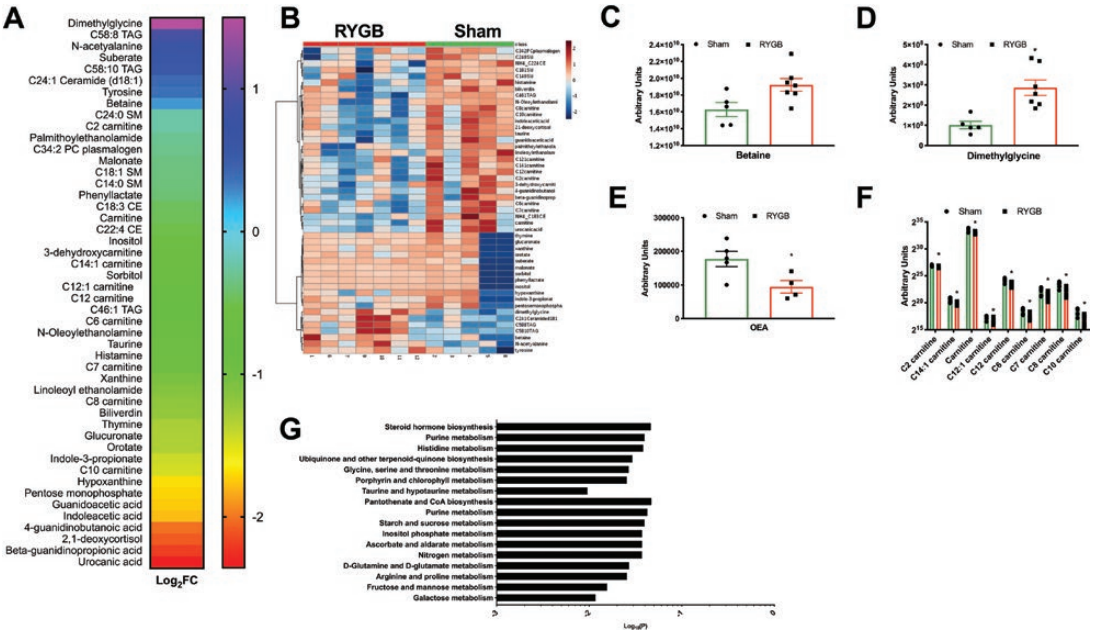

Figure 3. Portal metabolomic profiling. A, Log_2 fold-change in significantly affected systemic metabolites. B, Heat map showing log_2 fold-change in known portal metabolites found to differ significantly (as defined by $P < .05$) in portal blood from Roux-en-Y gastric bypass (RYGB) vs sham animals. C to D, B, Betaine and C, dimethylglycine (DMG) concentrations were increased in portal venous (PV) blood after RYGB. E, Portal N-oleoylethanolamide (OEA) levels were reduced by RYGB. F, Acylcarnitine levels were depleted. G, Pathway analysis revealed significant perturbation of several pathways, including hexose and disaccharide metabolism, nitrogen metabolism, and one-carbon metabolism (OCM). *P less than .05.

VIP scores greater than 1.0. The 15 metabolites with the highest VIP scores are shown in Fig. 4E; the top pathway distinguishing RYGB vs sham PV fingerprints was glycine/serine/threonine metabolism.

C. Comparison of Portal and Peripheral Blood Reveals Unique Portal Venous Metabolomic Profiling After Roux-en-Y Gastric Bypass

Portal blood demonstrated a unique metabolomic fingerprint distinct from that of peripheral blood (Fig. 5A and 5B). Linear regression analysis demonstrated no significant correlation of known metabolites (Fig. 5E; $R^2 = 0.002$, $P = .41$). PCA of 281 unique metabolites (excluding metabolites not detectable in all samples) from all 4 groups (peripheral RYGB, peripheral sham, portal RYGB, and portal sham) was performed, and we extracted the first 10 of 23 PCs describing the variance in our data (Fig. 5C). PC1 described most of the variance in our data, and was the major axis describing differences between portal and peripheral profiles. A total of 280 metabolites aligned with PC1, and these functionally contributed to arginine/proline metabolism, aminoacyl–transfer RNA biosynthesis, sphingolipid metabolism, glycine/serine/threonine metabolism, and branched-chain AA (BCAA) biosynthesis (Fig. 5D). This highlights the biology of the gut-liver axis, perhaps reflecting basal intestinal cell turnover (thus, affecting PV levels of sphingolipids and glycerophospholipids relative to peripheral blood) and AA metabolism within both the intestine and liver.

To determine which portal metabolites might be predicted by peripheral blood metabolites, we performed Pearson correlation between raw portal and peripheral metabolite levels for each metabolite. In our data set, DMG levels in peripheral and PV blood were strongly associated ($R = 0.88$, $P = .0001$, FDR-adjusted $P = .03$), suggesting parallel regulation of OCM in the intestine and liver. C47:1 TAG was also highly correlated ($R = 0.84$, $P = .001$, FDR-adjusted $P = .05$). Among those top anticorrelated metabolites were TAG species

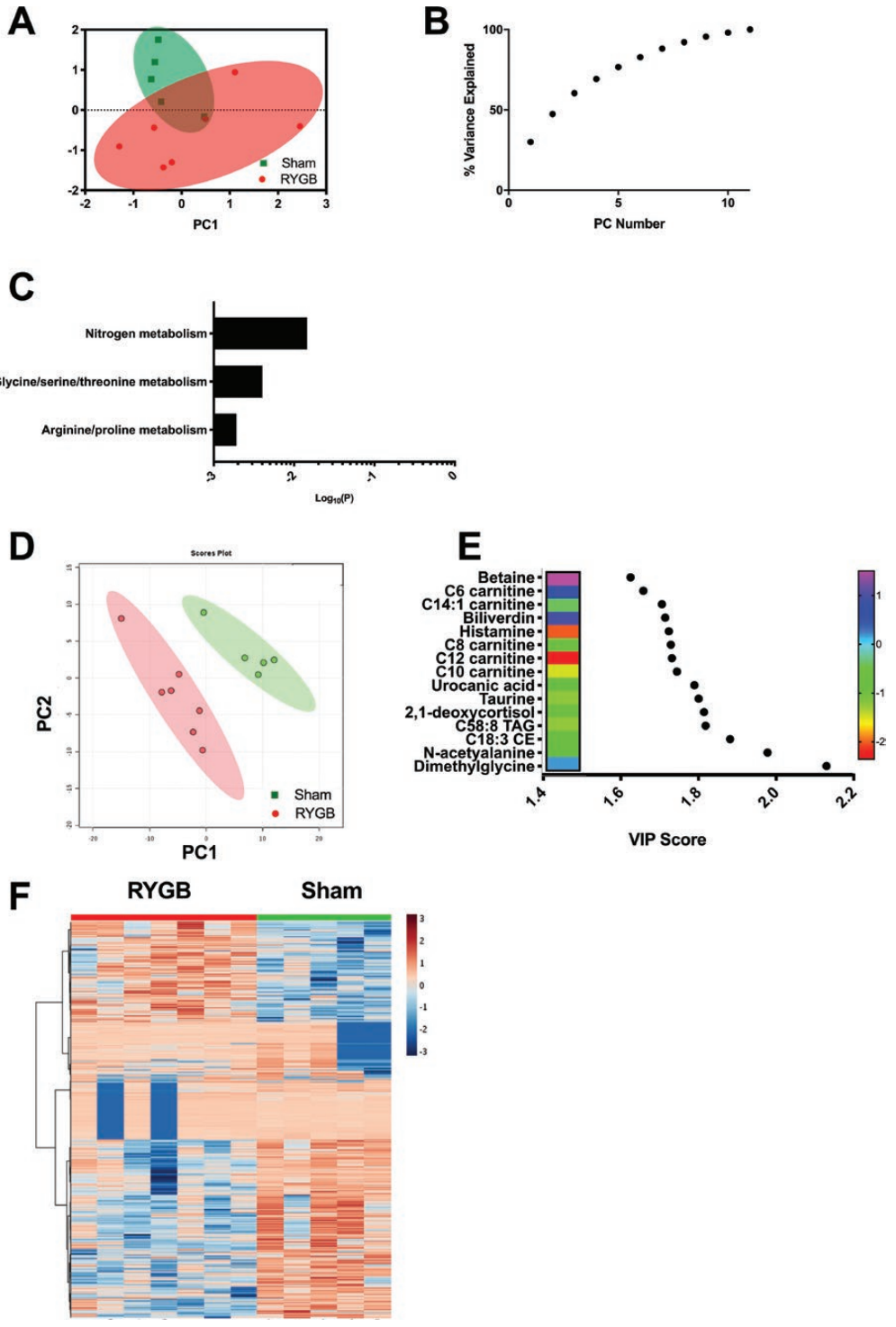

Figure 4. Portal venous metabolites distinguishing Roux-en-Y gastric bypass (RYGB)- from sham-operated animals. A, Principal components analysis (PCA) scores plot representing peripheral blood samples from RYGB- and sham-operated animals. B, Corresponding scree plot. C, PC2 contributed most significantly to the separation between the 2 groups and was enriched for metabolites found by pathway analysis to be important for glycine/serine/threonine metabolism, nitrogen metabolism, and arginine/proline metabolism. E, Top 15 metabolites identified by partial least squares discriminant analysis (PLS-DA) as key discriminating metabolites D), between the 2 experimental groups. E, Heat map shows $\log_2$ fold-change in identified metabolites, and all were significant as defined by P less than .05. F, Heat map demonstrating levels of unknown metabolites in RYGB- and sham-operated animals.

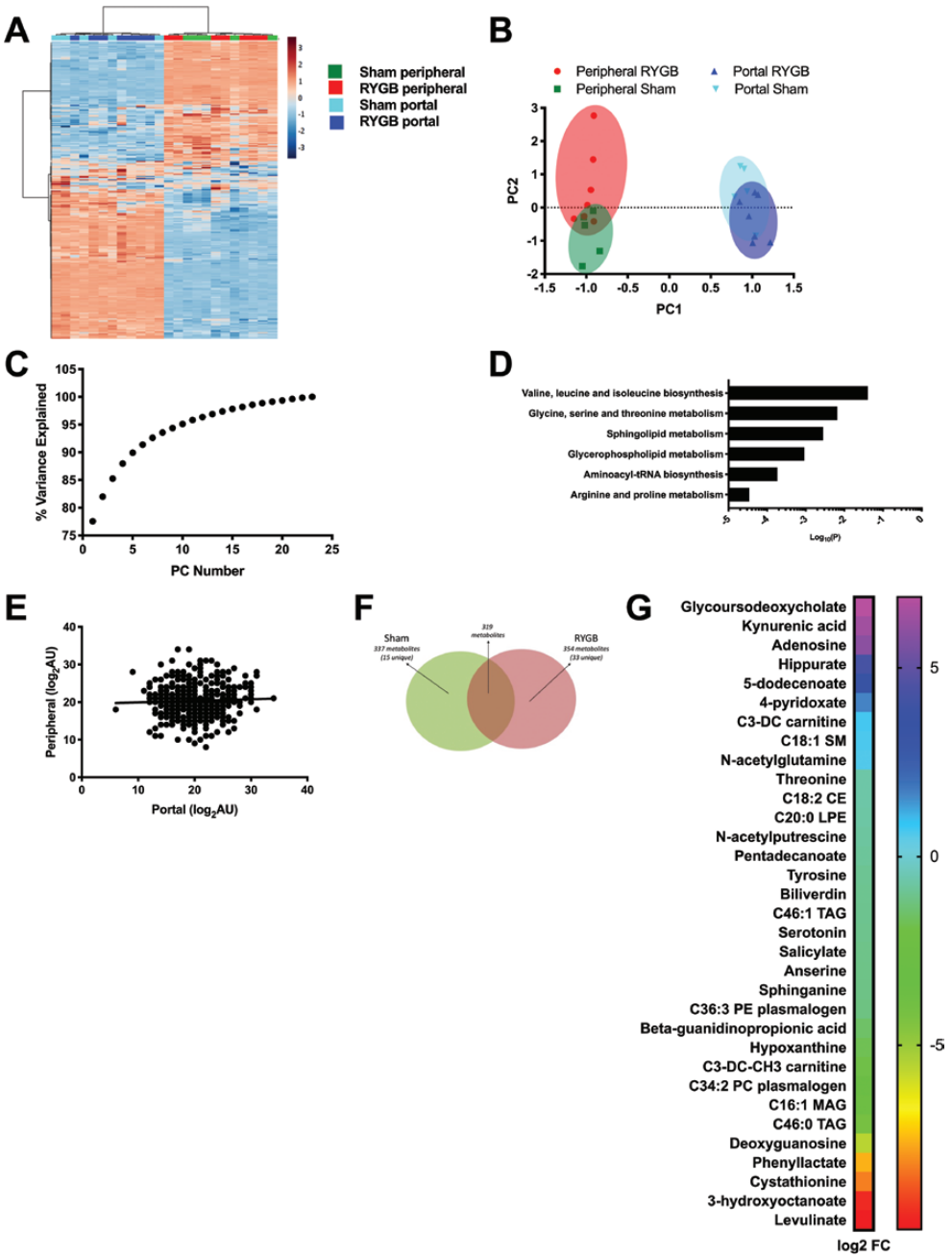

Figure 5. Portal and peripheral metabolomic signatures are distinct but for a subset of metabolites, portal concentration can be predicted by peripheral levels. A, Hierarchical clustering with heat mapping demonstrates clearly distinct metabolomic fingerprints in peripheral and portal blood, and less separation between Roux-en-Y gastric bypass (RYGB)- and sham-operated groups. B, Principal components analysis (PCA) scores plot demonstrating separation between blood compartments along PC1 axis. C, Scree plot demonstrating 23 PCs describing variance in data; based on this, we used a 10-factor solution to find those metabolites most aligned with PC1. D, Pathway analysis of PC1 metabolites demonstrates enrichment for several amino acid (AA) metabolic pathways including arginine/proline metabolism and branched-chain amino acid (BCAA) metabolism, sphingolipid, and glycerophospholipid metabolism and glycine/serine/threonine metabolism. E, No correlation was found between average metabolite levels in portal and peripheral blood. AU, arbitrary units. F, Of 354 metabolites significantly enriched or depleted in portal blood (as compared with systemic blood) after RYGB, 33 were uniquely affected after RYGB and not after sham surgery. G, Metabolites significantly enriched or depleted in portal venous blood from RYGB- but not sham-operated rats, as compared with in peripheral blood. Plotted is $\log_2$ fold-change (log(2)FC)).

(C50:6 TAG, R = –0.71, P = .009, FDR-adjusted P = .25; C54:9 TAG, R = –0.82, P = .001, FDR-adjusted P = .07); bilirubin (R = –0.73, P = .01, FDR-adjusted P = .23); and carnitine (R = –0.83, P = .001, FDR-adjusted P = .06), consistent with the liver being a key site for lipid, bile acid, and AA metabolism.

We identified 337 metabolites that were significantly altered in portal vs peripheral blood in sham-operated animals, and 354 metabolites that were significantly enriched or depleted in portal blood from RYGB-operated animals (Fig. 5F). Of these, 15 were uniquely affected in sham-operated animals and 33 in RYGB-operated animals (Fig. 5G). Pathway analysis of these 33 uniquely affected metabolites revealed overrepresentation of sphingolipid metabolism (P = .04), and ubiquinone and other terpenoid-quinone biosynthesis (P = .04).

D. Comparison to Roux-en-Y Gastric Bypass–Elicited Weight Loss in Humans

To ask how our findings relate to the metabolomic response to RYGB in obese humans, we next compared rodent peripheral blood to peripheral blood metabolomic signatures of 14 patients at least 6 months after RYGB surgery, vs 11 obese control patients. Of 66 metabolites in human serum that were significantly altered at least 6 months after RYGB as compared to control patients, 11 metabolites were also significantly altered in lean rats after RYGB (compared with sham; Fig. 6A). Metabolism of AAs including glycine/serine/threonine metabolism were among the most highly enriched pathways represented by these 11 metabolites (Fig. 6B and 6C).

4. Discussion

Data from our group [12, 13] and others [25, 26] highlight an important role for the gut-liver axis to contribute to the metabolic benefits of RYGB, including T2D remission. In this study, we performed PV metabolomic fingerprinting to shed light on metabolic changes elicited in the liver and intestine by RYGB. This was compared to peripheral metabolomic profiling to anchor our model of RYGB in lean animals, and to allow for comparison to what is known about human RYGB.

RYGB's effect on the PV metabolome is assumed to reflect alterations to intestinal physiology and metabolism. Our laboratory's prior work and data from others [25, 26] support a role for intestinal remodeling after RYGB to explain the surgery's dramatic clinical benefits including T2D remission. We have shown that, after RYGB, the Roux limb (RL) demonstrates evidence of proliferation and enhanced metabolism of metabolic fuels including glucose and AA [12, 13]. The findings from this study support these data and provide direct evidence of altered metabolic substrate use in the intestine. PV fingerprinting demonstrated alterations to nitrogen metabolism, which may reflect intestinal reprogramming after surgery. These changes could be due to changes to AA metabolism in intestinal tissue itself, or by gut microbiota; the latter in particular could explain changes to levels of essential AAs and their precursors. Importantly, we found that PV blood exhibits a distinct fingerprint relative to peripheral blood, reflecting its unique position as a carrier of metabolomic information from the intestine to the liver. Although several key pathways were influenced by RYGB in both compartments, this more likely represents similar use of certain substrates in liver and intestine, and overall the 2 signatures did not correlate and exhibited separation when the fingerprints were subjected to cluster analysis.

We demonstrated alteration in levels of several AAs after RYGB. However, although other reports have demonstrated reduction in circulating AA levels, particularly BCAA levels [14, 15, 18, 19], this was not the case in our study, in which we demonstrated increased levels of selected AAs. We speculate that this could be due to the lean model used for our experiment. In fact, obese individuals exhibit increased serum BCAA levels, and these levels are higher in insulin-resistant patients [27-29] and rodents [30]. RYGB appears to reverse this obesity-associated hyperaminoacidemia, but until now there has been no study that has tested whether AA levels fall independently of postsurgical weight loss and presurgical body mass

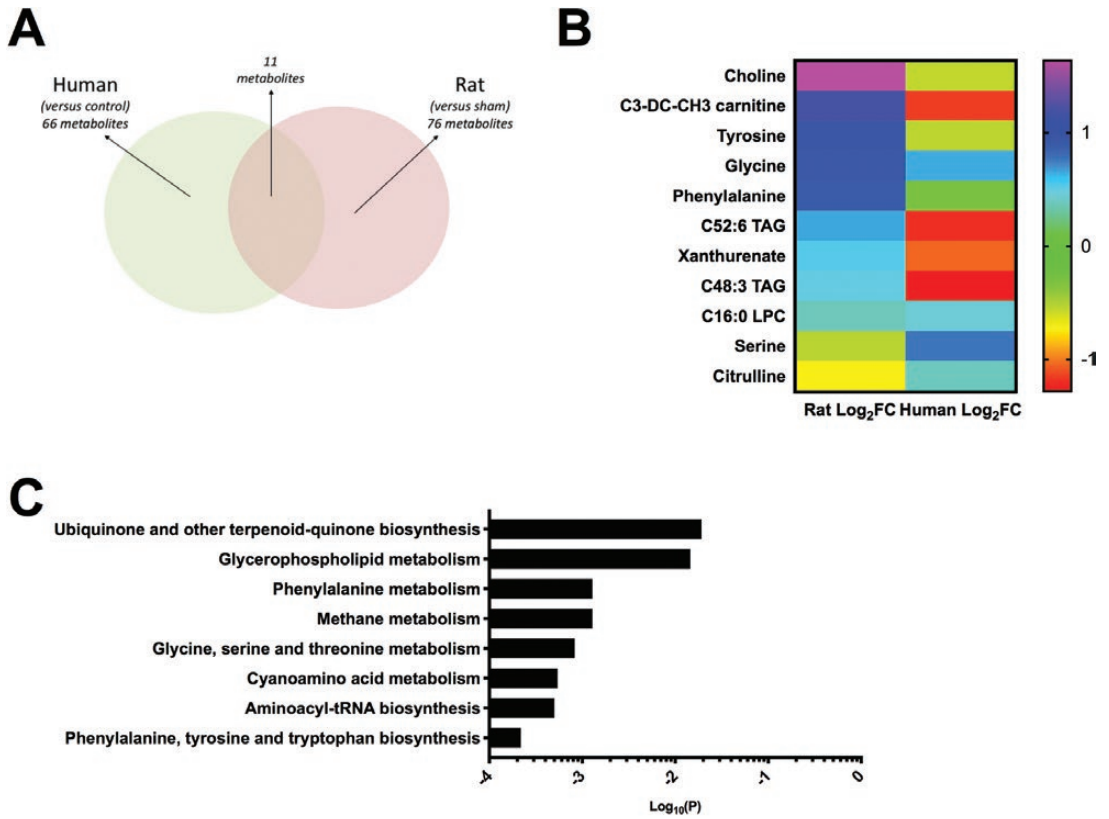

Figure 6. A, Venn diagram demonstrating that, of 76 metabolites significantly affected in peripheral blood of rats after Roux-en-Y gastric bypass (RYGB) (vs sham), and 66 metabolites significantly enriched or depleted in blood from human patients after RYGB as compared with control individuals, 11 metabolites were affected in both experiments. B, Eleven metabolites were significantly affected in peripheral blood after RYGB both in humans and rats. Plotted is $\log_2$ fold-change (log(2)FC). C, Pathway analysis of these 11 metabolites revealed overrepresentation of amino acid metabolism including glycine/serine/threonine metabolism, among other pathways.

index. Our study suggests that this is not the case, and that although RYGB does appear to influence nitrogen metabolism both in lean and obese states, the regulation may depend on the degree of obesity and/or insulin resistance present before surgery.

Although gluconeogenic AAs were, for the most part, unaffected in PV blood, several were enriched in peripheral samples, perhaps reflecting reduced hepatic use as gluconeogenic substrate, and suggesting that RYGB may blunt hepatic gluconeogenesis in a manner independently of weight loss. The liver plays a critical role in regulating whole-body glucose metabolism, and aberrant hepatic glucose metabolism is a key feature of T2D. Hepatic gluconeogenesis has been shown to be reduced by RYGB [31-33] and may be related to improved hepatic insulin sensitivity. Our laboratory's prior work demonstrated that RYGB elicits enduring changes to the hepatic transcriptomic fingerprint, which is distinct relative to the effect of caloric restriction [13], implying that these changes are not explained by weight loss or caloric restriction alone. The present study lends support to the concept of weight-loss–independent changes, given that blood was collected after animals had regained weight lost postoperatively.

Hepatic lipid metabolism is another key contributor to whole-body glucose homeostasis and may be entrained by PV metabolite messengers from the intestine. In this study, we found that the lipid messenger, OEA, was depleted in PV blood after RYGB. OEA is produced in the duodenum and jejunum in response to feeding, and serves as an activator of the nuclear receptor peroxisome proliferator-activated receptor α (PPARα). Importantly, OEA was identified as a weight-loss–independent metabolite, despite no

differences in dietary composition between the 2 groups and despite little to no reduction in food intake chronically after RYGB in rodents [7, 34]. We have previously reported that hepatic PPARα activity appears to be reduced chronically after RYGB as compared with caloric restriction, in tandem changes in hepatic lipid metabolism [13], thus positioning PPARα as a key transcriptional regulator that may elicit weight-loss–independent metabolic changes in response to the surgery. Our present findings shed light on a potential mechanistic role for reduced intestinal OEA production to entrain these changes in hepatic lipid metabolism, perhaps through PPARα. We hypothesize that reduced PV OEA concentrations may relate to exclusion of the biliopancreatic limb (duodenum) from the flow of nutrient delivery because there was no difference in nutrient intake between the 2 experimental groups.

OCM was found to be altered both in portal and peripheral compartments. Notably, glycine/serine/threonine metabolism was enriched in both locations, and was the top pathway distinguishing RYGB from sham metabolite profiles in PV blood. The choline degradation product, DMG, was enriched both in portal and peripheral blood after RYGB, and the fact that DMG was more dramatically affected in portal blood may contribute to an understanding of why changes in OCM also explained differences between portal and peripheral profiles. We hypothesize that OCM, as an important means for folate donation and thus for methylation, as a key regulatory pathway for gene silencing, may link metabolic changes within the intestine and liver to local changes in gene expression. This could possibly provide a mechanism linking changes in luminal nutrient flow as a result of the surgery to long-term adaptations within the tissue. It may also explain the changes in blood and skeletal muscle methylation levels observed by other groups [35, 36] after surgery. Finally, based on the fact that depletion of the methyl donors choline and methionione results in hepatic lipid accumulation resembling nonalcoholic fatty liver disease (NAFLD) [37, 38], we hypothesize that enrichment of DMG and betaine in PV blood might relate mechanistically to improvements in NAFLD after RYGB. Importantly, we also found that OCM was enriched in peripheral blood from obese patients after RYGB, signifying that this may be important not only in the case of the lean rodents studied here. However, further study is needed to understand the potential mechanistic role of OCM in the amelioration of metabolic disease including NAFLD after bariatric surgery.

This study is the first to use untargeted metabolomic profiling to characterize the PV metabolite fingerprint after RYGB. It is important to note that LC-MS does not allow for distinction between certain very similar metabolites such as certain hexoses. However, this technology is very sensitive, broad, and robust and considered superior to other analysis methods. We do recognize that significant findings from this study may need to be validated on another platform to confirm specificity for highlighted metabolites, but this study provides an important glimpse into the effects of RYGB on metabolism in the gut-liver axis, and fills an essential gap in our knowledge about how alterations in intestinal biology might entrain changes in hepatic metabolism. A strength of this study is the use of an animal model to overcome a technical barrier limiting PV sampling in humans and additionally to remove the confounding variables of obesity and weight loss from the experimental design. Although only male rats were used in this study, the male rat is an ideal model for RYGB in humans and bariatric surgery has been modeled mostly in male rodents. This is largely related to the fact that females are more protected against diet-induced obesity [39].

In conclusion, in the portal vein, which is the key humoral communication route between the intestine and liver, RYGB elicits key changes in nitrogen in OCM that are independent of weight loss after surgery. We hypothesize that these might link known changes in intestinal and hepatic physiology after RYGB, and that changes in folate metabolism might relate to epigenetic reprogramming of both organs as a mechanism for the beneficial effects of RYGB that have been shown to persist beyond the effects of dieting. Together, these data uncover critical insight into how the surgery influences the gut-liver axis and shed light on potential mechanisms for future study in animals and in humans.

Acknowledgments

We would like to thank Ms Courtney Panciotti for her technical assistance.

Financial Support: This work was supported by National Institutes of Health grants 5K12KD094721 (to M.A.S.) and 5R01KD10842 (to N.S.).

Author Contributions: M.A.S. and N.S. conceived of and designed the study. M.A.S. performed and led the analysis. Discussions with N.S., J.A.P., and C.C. were integral to the study design and data interpretation. Acquisition and processing of raw data was performed by J.A.P., K.B. (C18-negative data), K.P. (HILIC-negative data), and A.D. (C8-positive data).

Additional Information

Correspondence: Margaret A. Stefater, MD, PhD, Division of Endocrinology, Boston Children's Hospital, 300 Longwood Avenue, Boston, Massachusetts 02115. E-mail: margaret.stefater@childrens.harvard.edu.

Disclosure Summary: The authors have nothing to disclose.

Data Availability: All data generated or analyzed during this study are included in this published article or in the data repositories listed in References.

References and Notes

1. Ahmed B, King WC, Gourash W, et al. Long-term weight change and health outcomes for sleeve gastrectomy (SG) and matched Roux-en-Y gastric bypass (RYGB) participants in the Longitudinal Assessment of Bariatric Surgery (LABS) study. *Surgery*. 2018;**164**(4):774–783.
2. Courcoulas AP, King WC, Belle SH, et al. Seven-year weight trajectories and health outcomes in the Longitudinal Assessment of Bariatric Surgery (LABS) study. *JAMA Surg*. 2018;**153**(5):434.
3. Courcoulas AP, Belle SH, Neiberg RH, et al. Three-year outcomes of bariatric surgery vs lifestyle intervention for type 2 diabetes mellitus treatment: a randomized clinical trial. *JAMA Surg*. 2015;**150**(10):931–940.
4. Inge TH, Courcoulas AP, Jenkins TM, et al; Teen-LABS Consortium. Weight loss and health status 3 years after bariatric surgery in adolescents. *N Engl J Med*. 2016;**374**(2):113–123.
5. Inge TH, Miyano G, Bean J, et al. Reversal of type 2 diabetes mellitus and improvements in cardiovascular risk factors after surgical weight loss in adolescents. *Pediatrics*. 2009;**123**(1):214–222.
6. Zakeri R, Batterham RL. Potential mechanisms underlying the effect of bariatric surgery on eating behaviour. *Curr Opin Endocrinol Diabetes Obes*. 2018;**25**(1):3–11.
7. Stefater MA, Wilson-Pérez HE, Chambers AP, Sandoval DA, Seeley RJ. All bariatric surgeries are not created equal: insights from mechanistic comparisons. *Endocr Rev*. 2012;**33**(4):595–622.
8. Hutch CR, Sandoval D. The role of GLP-1 in the metabolic success of bariatric surgery. *Endocrinology*. 2017;**158**(12):4139–4151.
9. Liou AP, Paziuk M, Luevano JM Jr, Machineni S, Turnbaugh PJ, Kaplan LM. Conserved shifts in the gut microbiota due to gastric bypass reduce host weight and adiposity. *Sci Transl Med*. 2013;**5**(178):178ra41.
10. Osto M, Abegg K, Bueter M, le Roux CW, Cani PD, Lutz TA. Roux-en-Y gastric bypass surgery in rats alters gut microbiota profile along the intestine. *Physiol Behav*. 2013;**119**:92–96.
11. Fouladi F, Brooks AE, Fodor AA, et al. The role of the gut microbiota in sustained weight loss following Roux-en-Y gastric bypass surgery. *Obes Surg*. 2019;**29**(4):1259–1267.
12. Saeidi N, Meoli L, Nestoridi E, et al. Reprogramming of intestinal glucose metabolism and glycemic control in rats after gastric bypass. *Science*. 2013;**341**(6144):406–410.
13. Ben-Zvi D, Meoli L, Abidi WM, et al. Time-dependent molecular responses differ between gastric bypass and dieting but are conserved across species. *Cell Metab*. 2018;**28**(2):310–323.e6.
14. Laferrère B, Reilly D, Arias S, et al. Differential metabolic impact of gastric bypass surgery versus dietary intervention in obese diabetic subjects despite identical weight loss. *Sci Transl Med*. 2011;**3**(80):80re2.
15. Mutch DM, Fuhrmann JC, Rein D, et al. Metabolite profiling identifies candidate markers reflecting the clinical adaptations associated with Roux-en-Y gastric bypass surgery. *Plos One*. 2009;**4**(11):e7905.
16. Lips MA, Van Klinken JB, van Harmelen V, et al. Roux-en-Y gastric bypass surgery, but not calorie restriction, reduces plasma branched-chain amino acids in obese women independent of weight loss or the presence of type 2 diabetes. *Diabetes Care*. 2014;**37**(12):3150–3156.

17. Magkos F, Bradley D, Schweitzer GG, et al. Effect of Roux-en-Y gastric bypass and laparoscopic adjustable gastric banding on branched-chain amino acid metabolism. *Diabetes*. 2013;**62**(8):2757–2761.
18. Lopes TI, Geloneze B, Pareja JC, Calixto AR, Ferreira MM, Marsaioli AJ. Blood metabolome changes before and after bariatric surgery: a (1)H NMR-based clinical investigation. *OMICS*. 2015;**19**(5):318–327.
19. Arora T, Velagapudi V, Pournaras DJ, et al. Roux-en-Y gastric bypass surgery induces early plasma metabolomic and lipidomic alterations in humans associated with diabetes remission. *PloS One*. 2015;**10**(5):e0126401.
20. Mazzini GS, Khoraki J, Dozmorov M, et al. Concomitant PPARα and FXR activation as a putative mechanism of NASH improvement after gastric bypass surgery: a GEO datasets analysis. *J Gastrointest Surg*. 2019;**23**(1):51–57.
21. Sacks J, Mulya A, Fealy CE, et al. Effect of Roux-en-Y gastric bypass on liver mitochondrial dynamics in a rat model of obesity. *Physiol Rep*. 2018;**6**(4):e13600.
22. Pardina E, Ferrer R, Rossell J, et al. Hepatic CD36 downregulation parallels steatosis improvement in morbidly obese undergoing bariatric surgery. *Int J Obes (Lond)*. 2017;**41**(9):1388–1393.
23. Esko T, Hirschhorn JN, Feldman HA, et al. Metabolomic profiles as reliable biomarkers of dietary composition. *Am J Clin Nutr*. 2017;**105**(3):547–554.
24. Abidi W, Nestoridi E, Feldman H, et al. Differential metabolomic signatures in patients with weight regain and sustained weight loss after gastric bypass surgery: a pilot study. [Published online ahead of print August 5, 2019.] *Dig Dis Sci*. Doi: 10.1007/s10620-019-05714-3
25. Cavin JB, Couvelard A, Lebtahi R, et al. Differences in alimentary glucose absorption and intestinal disposal of blood glucose after Roux-en-Y gastric bypass vs sleeve gastrectomy. *Gastroenterology*. 2016;**150**(2):454–464.e9.
26. Magkos F, Bradley D, Eagon JC, Patterson BW, Klein S. Effect of Roux-en-Y gastric bypass and laparoscopic adjustable gastric banding on gastrointestinal metabolism of ingested glucose. *Am J Clin Nutr*. 2016;**103**(1):61–65.
27. Newgard CB, An J, Bain JR, et al. A branched-chain amino acid-related metabolic signature that differentiates obese and lean humans and contributes to insulin resistance. *Cell Metab*. 2009;**9**(4):311–326.
28. Tai ES, Tan ML, Stevens RD, et al. Insulin resistance is associated with a metabolic profile of altered protein metabolism in Chinese and Asian-Indian men. *Diabetologia*. 2010;**53**(4):757–767.
29. Felig P, Marliss E, Cahill GF Jr. Plasma amino acid levels and insulin secretion in obesity. *N Engl J Med*. 1969;**281**(15):811–816.
30. She P, Van Horn C, Reid T, Hutson SM, Cooney RN, Lynch CJ. Obesity-related elevations in plasma leucine are associated with alterations in enzymes involved in branched-chain amino acid metabolism. *Am J Physiol Endocrinol Metab*. 2007;**293**(6):E1552–E1563.
31. Dunn JP, Abumrad NN, Breitman I, et al. Hepatic and peripheral insulin sensitivity and diabetes remission at 1 month after Roux-en-Y gastric bypass surgery in patients randomized to omentectomy. *Diabetes Care*. 2012;**35**(1):137–142.
32. Immonen H, Hannukainen JC, Iozzo P, et al. Effect of bariatric surgery on liver glucose metabolism in morbidly obese diabetic and non-diabetic patients. *J Hepatol*. 2014;**60**(2):377–383.
33. Yan Y, Zhou Z, Kong F, et al. Roux-en-Y gastric bypass surgery suppresses hepatic gluconeogenesis and increases intestinal gluconeogenesis in a T2DM rat model. *Obes Surg*. 2016;**26**(11):2683–2690.
34. Saeidi N, Nestoridi E, Kucharczyk J, Uygun MK, Yarmush ML, Stylopoulos N. Sleeve gastrectomy and Roux-en-Y gastric bypass exhibit differential effects on food preferences, nutrient absorption and energy expenditure in obese rats. *Int J Obes (Lond)*. 2012;**36**(11):1396–1402.
35. Barres R, Kirchner H, Rasmussen M, et al. Weight loss after gastric bypass surgery in human obesity remodels promoter methylation. *Cell Rep*. 2013;**3**(4):1020–1027.
36. Kirchner H, Nylen C, Laber S, et al. Altered promoter methylation of PDK4, IL1 B, IL6, and TNF after Roux-en Y gastric bypass. *Surg Obes Relat Dis*. 2014;**10**(4):671–678.
37. Zhang BH, Weltman M, Farrell GC. Does steatohepatitis impair liver regeneration? A study in a dietary model of non-alcoholic steatohepatitis in rats. *J Gastroenterol Hepatol*. 1999;**14**(2):133–137.
38. Weltman MD, Farrell GC, Liddle C. Increased hepatocyte CYP2E1 expression in a rat nutritional model of hepatic steatosis with inflammation. *Gastroenterology*. 1996;**111**(6):1645–1653.
39. Dakin RS, Walker BR, Seckl JR, Hadoke PW, Drake AJ. Estrogens protect male mice from obesity complications and influence glucocorticoid metabolism. *Int J Obes (Lond)*. 2015;**39**(10):1539–1547.